XVIII International Conference on Water Resources
CMWR 2010
J. Carrera (Ed)
CIMNE, Barcelona 2010

PORE SCALE MODELING OF TWO-PHASE FLOW

Vahid Shabro[*], Maša Prodanović[*], Christoph H. Arns[†], Steven L. Bryant[*], Carlos Torres-Verdin[*], and Mark A. Knackstedt[#]

[*] Department of Petroleum and Geosystems Engineering, University of Texas at Austin,
1 University Station, C0300, Austin, TX 78712, USA
e-mails: vshabro@mail.utexas.edu, masha@ices.utexas.edu, steven_bryant@mail.utexas.edu,
cverdin@uts.cc.utexas.edu

[†] School of Petroleum Engineering, University of New South Wales,
Sydney NSW 2052, Australia
e-mail: c.arns@unsw.edu.au

[#]Department of Applied Mathematics, Research School of Physical Sciences and Engineering,
Australian National University, Canberra, Australia
e-mail: mak110@rsphy1.anu.edu.au

Key words: porous media, absolute and relative permeability, drainage, formation factor

Summary. In this paper, we compare predictions of several pore-scale codes for single- and two-phase flow for the first time. Firstly, two implementations of lattice-Boltzmann method (LBM) and a finite-difference based code (FDDA) predict single-phase flow in Fontainebleau sandstone and dolomite samples. We then obtain pore-scale drainage for two fluid phase configurations using a novel level set method based progressive quasi-static (LSMPQS) algorithm for capillarity dominated flow. The resulting fluid configurations are used to compute relative permeability using LBM in each phase as well as formation factor. We demonstrate that the numerical methods compare well with each other and available experimental results.

1 INTRODUCTION

High-resolution, three-dimensional, X-ray microtomography images of multiphase porous media have become widely available over the past decade [1,2]. At the same time, several methods have been developed to both analyze the imaged pore space and calculate macroscopic flow properties [3-6]. Absolute and relative permeability are regarded as the most fundamental pore-scale properties [7] since they are inputs to large-scale reservoir simulations and are the basis for any modeling/prediction of more complex/coupled phenomena. The objective of this paper is to validate methods to calculate image-based permeability.

When modeling flow in porous media with the objective of estimating macroscopic flow properties such as permeability, one has a choice of network modeling or direct simulation in the imaged pore space. Network modeling (for an overview see [8,9]) requires non-trivial processing of the imaged pore space [10-13] to derive a representative network of geometrically simplified pores (openings) and throats (constrictions). In this paper, we focus on direct methods. Lattice Boltzmann method [14] (LBM) is by now a well-established method for permeability estimations. Two-phase lattice Boltzmann implementations in porous materials are reported by a number of research groups [15,16], however they require intensive parallel computational resources.

Understanding the relative permeability (flow conductivity to a phase in the presence of others) is crucial in describing flow in most subsurface systems. Relative permeability, however, is very sensitive to fluid configurations in space (as opposed to depending on the saturation only). Since two-phase Navier Stokes simulations in porous media are computationally demanding, a number of methods have sought to circumvent them [17]. In either drainage or imbibition, fluid-fluid interface geometry (that ultimately determines fluid configurations) is dominated by capillary forces (interfacial tension) on the length scales smaller than millimeter and the influences of viscosity and gravity can be neglected. The complex pore space geometry together with capillary forces leads to a multitude of history dependent possibilities, including disconnections of either wetting or non-wetting phases. Methods such as invasion percolation [18] or maximal inscribed spheres [19] use inscribed radius information at each point of the pore space in order to obtain fluid configurations. They are fast and reasonably accurate methods for drainage fluid configurations by inherently assuming simplified spherical interfaces. We have recently developed a quasi-static drainage and imbibition fluid configurations based on the level set method [20]. This algorithm also works in the imaged pore space of arbitrary complexity, but makes no assumptions on the shape of the interface, i.e. finds correct capillarity-dominated interfaces. In terms of computational complexity, it is not as fast as invasion percolation methods but is faster than two-phase LBM methods.

Theoretical convergence estimates and validation of numerical approaches for Navier-Stokes flow to date remain impractical to model natural porous formations. We first compare lattice-Boltzmann and finite-difference based codes for simulation of single-phase flow in realistic samples independently developed by our respective research groups. Then, we estimate relative permeability using single-phase flow simulators in each of the fluid phases. Even though the estimated two-phase relative permeability does not explicitly incorporate inter-phase exchange of momentum, its computational complexity is within our current computational capacity in contrast with complexities of explicit two-phase flow simulations. Silin and Patzek [17] have similarly utilized drainage fluid configurations obtained from maximal inscribed spheres method. We further use the fluid configurations to compute the water phase conductivity (formation factor). The combination of experimental validation and cross-validation of different numerical approaches for estimation of properties is an important step toward more reliable modeling.

2 METHODS

2.1. Single phase permeability

Lattice Boltzmann method. The fluid flow in porous media can be calculated in steady-state condition, for an incompressible, Newtonian fluid in the limit of low Reynolds number (creeping flow) using Lattice-Boltzmann method (D3Q19 lattice). We solve the Stokes' and the mass conservation equations in the interstitial space of porous media

$$\mu\nabla^2 u = \nabla P \text{ and} \tag{1}$$

$$\nabla \cdot u = 0, \tag{2}$$

where μ is the viscosity, P the pressure and u is the local velocity. The corresponding permeability is calculated by comparing flow flux with Darcy's law. We enforce no-slip and no-penetration boundary conditions at the pore-grain surfaces. We compare two different implementations: (1) UT Austin's Pore-Level Petrophysics Toolbox (PLPT) 1.00 [21], with LBM details described in [22,23] with relaxation parameter τ=0.65. This implementation we refer to as **LBM/PLPT**. (2) MPI parallel implementation (which we refer to as **LBM/MPI**) [24,25] with relaxation parameter τ=1 and a second-order accurate mid-point style reflection rule for internal boundaries. LBM/PLPT sets inlet and outlet pressures, while LBM/MPI considers two macroscopic boundary conditions: mirroring of the structure in flow direction with periodic boundaries perpendicular to flow, and periodic boundary conditions with a free fluid padding layer of 15 voxel effectively making the sample periodic. No body force is applied outside the measuring window (the fluid pad).

Finite-difference diffusive-advective method (FDDA). We assume creeping flow in a porous medium and neglect compressibility in the small samples under investigation. Fluid flow consists of diffusive and advective parts and is solved via finite-difference method [26,27]. The advective flow applies the proper slip or no-slip boundary condition depending on throat sizes. The summation of these contributions to the flow results in

$$J = -\left(\frac{2r}{3RT}\left(\frac{8RT}{\pi M}\right)^{0.5} + F\frac{r^2\rho_{avg}}{8\mu}\right)\frac{(P_2 - P_1)}{L}, \tag{3}$$

where J is mass flux, r is the tube radius, R is the universal gas constant, T is temperature, M is the molar mass, ρ_{avg} is the average density at p_{avg}[=(P_1+P_2)/2], μ is the viscosity, P_1 and P_2 are pressures at the inlet and outlet of the tube, respectively, and L in the length of the tube. Coefficient F stands for the contribution of slip flow on a solid matrix surface. In this paper, the coefficient F is approximately equal to 1 since the grid sizes are in the micrometer range (i.e. the slip flow is not significant). If the contribution of the diffusive term is also neglected, Eq. (1) reduces to the Hagen–Poiseuille's equation. We impose pressure boundary conditions on inlet/outlet and no-penetration at the grain boundaries. We solve the resulted generalized Laplace equation in the form of

$$\nabla \cdot d\nabla P = 0\,, \tag{4}$$

where *d* is a weight factor calculated for each voxel according to its position in the pore space. This results in pressure and subsequently fluid velocities in the interstitial space. The permeability is again calculated by comparison to Darcy's law.

2.2. Two-phase fluid configurations: Level Set Method Progressive Quasistatic Algorithm (LSMPQS)

We obtain detailed pore level interface description at different saturations in arbitrary geometries for either a drainage or imbibition process. (see [20,28] and references therein). Numerical results are extensions of the publicly available code [29]. A short summary of the approach is as follows. The moving surface of interest is embedded as the zero level set of function $\phi(\vec{x},\tau)$ defined on entire domain and τ is a time-like parameter that tracks the motion of the interface toward an equilibrium position. The zero level set is the set of points $\vec{x}$ such that $\phi(\vec{x},\tau)=0$. Such representation enables elegant calculation of various interface properties. For instance, the normal to the interface is simply $\vec{n}=\frac{\nabla\phi}{|\nabla\phi|}$, where $\nabla\phi=(\phi_x,\phi_y,\phi_z)$ is the spatial gradient of ϕ, and (twice the) mean curvature κ is divergence of the normal. In level set methods, the level set function evolves in time according to the following partial differential equation:

$$\phi_\tau + F|\nabla\phi| = 0, \quad \phi(x,0)\ given \qquad , \tag{5}$$

where *F* is the speed of the interface in normal direction. More general equation is

$$\phi_\tau + \vec{u}\cdot\nabla\phi = 0, \quad \phi(x,0)\ given \qquad , \tag{6}$$

where $\vec{u}$ is external velocity field (if $\vec{u}=F\vec{n}=F\frac{\nabla\phi}{|\nabla\phi|}$, we will obtain previous equation). In the most general two phase flow application, one would propagate the fluid-fluid interface using velocity field $\vec{u}$ obtained by solving the Navier-Stokes equation. If capillarity is the dominant force, however, the interface at equilibrium will curve itself while balancing capillary pressure and interfacial tension (Young-Laplace equation $p_c=\sigma\kappa$). Thus the appropriate normal speed model at the core of slow, quasi-static interface movement is

$$F(\vec{x},\tau)=p_c-\sigma\kappa(\vec{x},\tau) \qquad . \tag{7}$$

We model the situation where the wetting fluid is perfectly wetting the solid surface (contact angle zero). This is effectively done describing the solid phase with a separate level set function and implementing a simple penalization if the meniscus enters the solid phase.

2.3. Water phase conductivity calculations

FD and FEM implementations. Conductivity is calculated by solving the generalized Laplace equation by either a finite difference method using an average of parallel and serial local conductivities to turn the voxel image into a network of resistors or a finite element

method (FEM) using parallel conductivity rules only [30]. The latter typically leads to smoother convergence. We will present comparisons with a random-walk implementation [23] in future.

3 RESULTS

We use a Fontainebleau sandstone, and a sucrosic dolomite 500^3 images with voxel length of 3.5 µm. Details on the samples are available in [31]. Figure 1 shows porosity variation for the subsamples used in this paper. Subsamples with 250 voxels on side show reasonable uniformity with respect to porosity and are considered practically representative of the larger image.

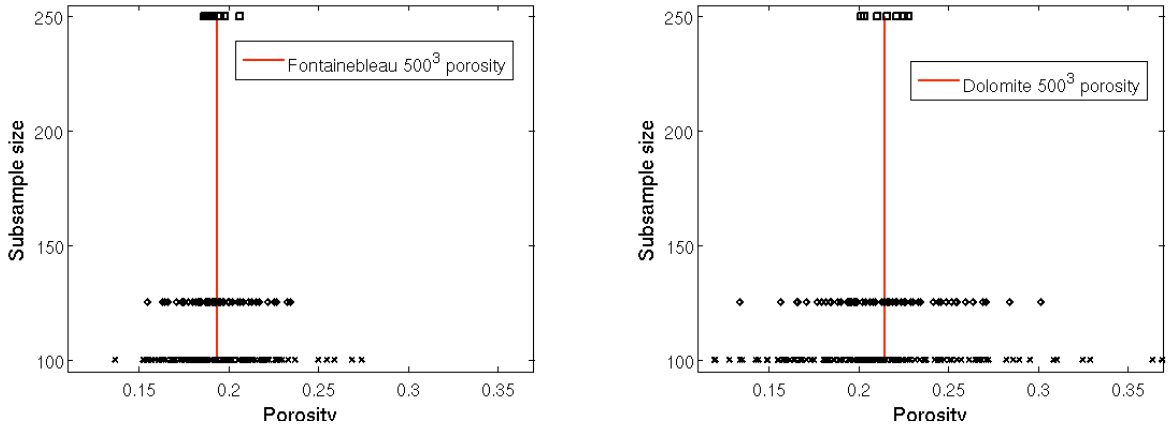

Figure 1: Porosity variation for subsamples of 500^3 Fontainebleau sandstone and dolomite images.

Single phase permeability. The results from the different methods indicate errors within 20% range in all cases under investigation (Figure 2). The modeling results are in agreement with the experimental values on larger, sister samples of the imaged ones, K=3 D for Fontainebleau sandstone and K=0.9 D in dolomite [31].

We observe that FDDA has an advantage over LBM in low resolution images. Tortuous paths with tight connections and unfavorable orientation compared with the global pressure gradient (implemented as a body force) might yield zero permeability in LBM while the actual permeability is small but finite. In contrast, FDDA checks all possible connections from the inlet to the outlet [26].

Drainage fluid configurations, relative permeability and conductivity. Figure 3 shows two cases for drainage in Fontainebleau and dolomite 250^3 samples. In part (a) non-wetting (NW) phase in Fontainebleau at the drainage step where the NW phase percolated to the opposite side and in part (b) trapped residual wetting (W) phase in dolomite are shown. Main advantage of using LSMPQS is easy handling of trapped phases. While we show only W phase trapping at drainage (Figure 3b), NW phase trapping at imbibition is also handled in this method [32], and to our knowledge LSMPQS is the only method to successfully match experimentally observed NW phase trapping. We will report on detailed trapping comparison

and the imbibition results in the future. Figure 4a shows curvature (equivalent to capillary pressure) saturation relationships. Non-smooth dolomite drainage curve indicates that a larger sample should be used for a better representation. We will address this issue in the future. Residual water phase saturation is much higher in dolomite than in the sandstone. The relative permeability computed from corresponding fluid configurations with different methods match well (Figure 4b). Conductivity of the samples is computed using FD/FEM implementation. We observe formation factor of 13.2 in Fontainebleau and 37.5 in dolomite 250^3 samples.

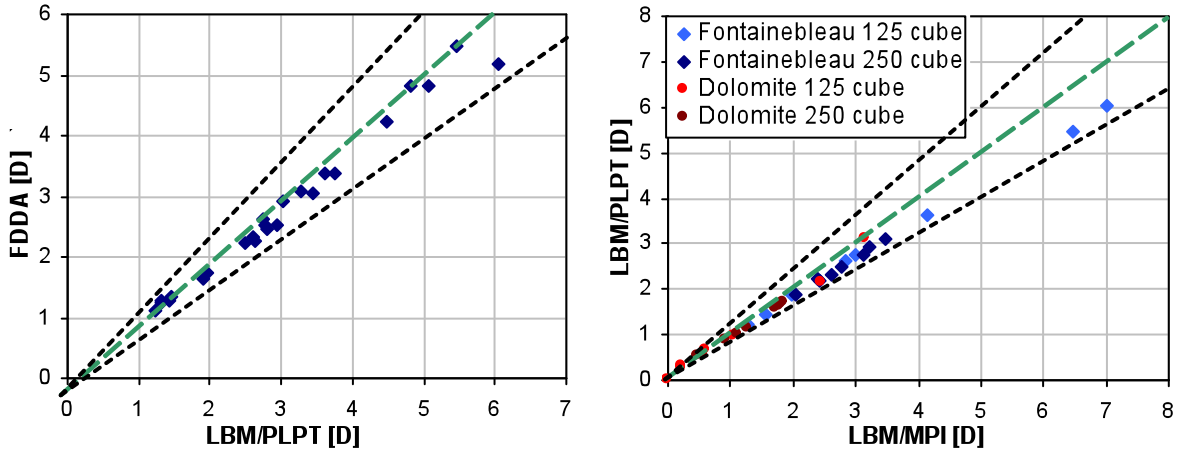

(a) (b)

Figure 2: Comparison between the absolute permeability results of a) FDDA and LBM/PLPT for the 125^3 images of Fontainebleau sandstone, and b) Two respective LBM implementations. The green dashed line shows the perfect match line and the dotted black lines are 20% relative error lines.

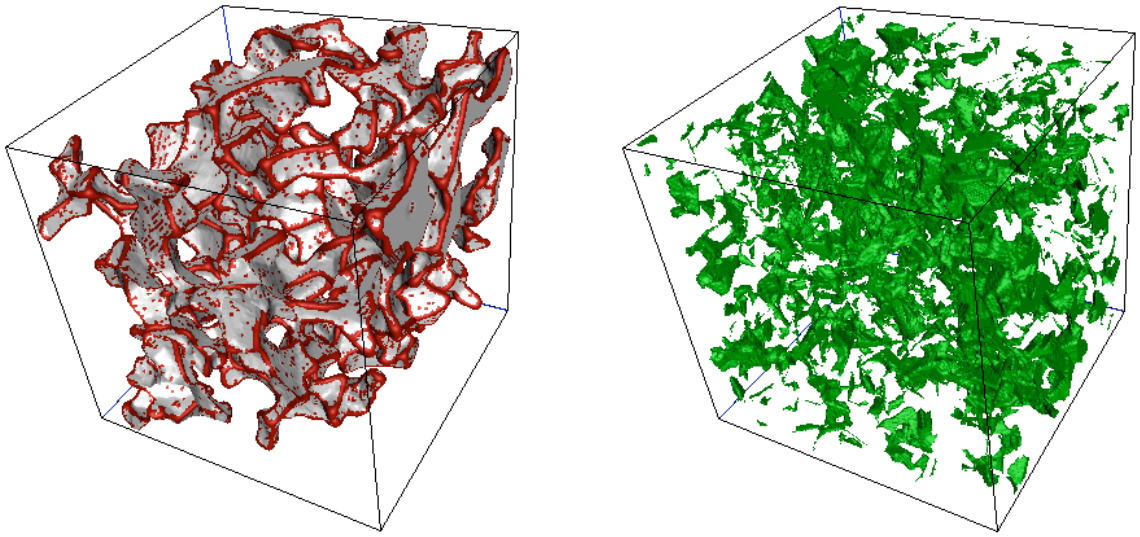

(a) (b)

Figure 3: (a) NW phase configuration in a Fontainebleau sandstone subsample (a 250^3 image) at the percolating drainage step. The NW-W fluid contact is colored red, and the NW-solid contact is colored gray. The drainage started from the face in the back. (b) Trapped residual wetting phase in the dolomite subsample at the end of drainage, S_{wr}=26% (cf. the experimental value of S_{wr}=22%).

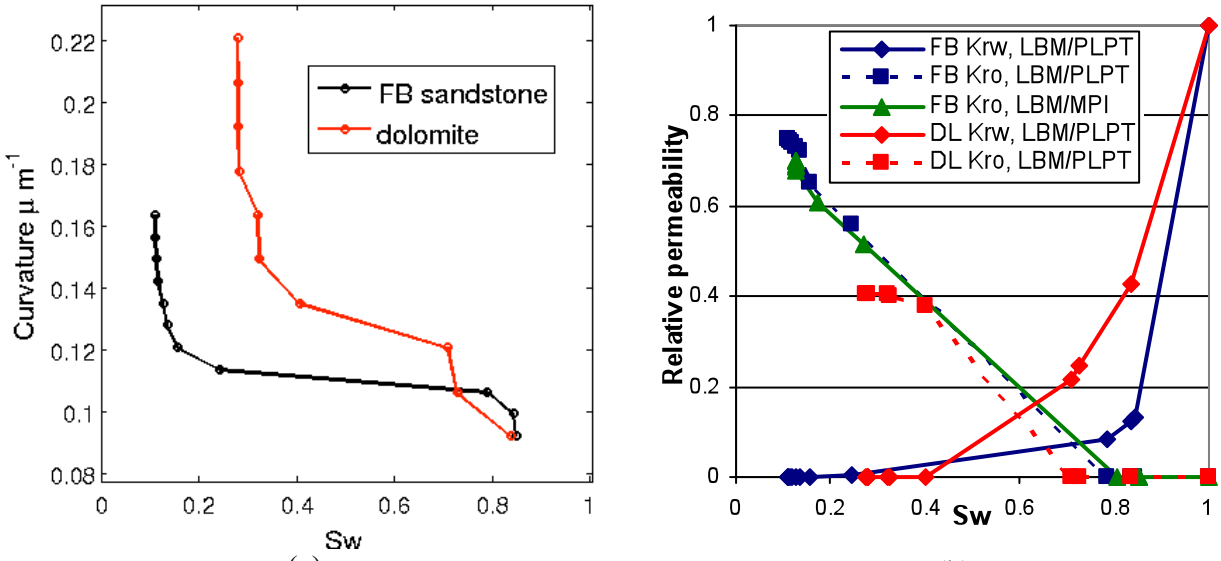

Figure 4: (a) Curvature-saturation curve for both Fontainebleau sandstone and dolomite samples. (b) Relative permeability results for the Fontainebleau (FB) and dolomite (DL) 250^3 drainage samples with 19.3% and 18.9% porosities respectively. The oil relative permeability is performed by both LBM/PLPT and LBM/MPI and the results are in agreement.

REFERENCES

[1] B.P. Flannery, H.W. Deckman, W.G. Roberge, and K.L. D'Amico, "Three-Dimensional X-Ray Microtomography," *Science*, vol. 237, 1987, pp. 1439–1444.

[2] D. Wildenschild, C.M.P. Vaz, M.L. Rivers, D. Rikard, and B.S.B. Christensen, "Using X-ray computed tomography in hydrology: systems, resolutions, and limitations," *Journal of Hydrology*, vol. 267, Oct. 2002, pp. 285-297.

[3] P. ØREN and S. Bakke, "Process Based Reconstruction of Sandstones and Prediction of Transport Properties," *Transport in Porous Media*, vol. 46, Feb. 2002, pp. 311-343.

[4] M.L. Turner, L. Knüfing, C.H. Arns, A. Sakellariou, T.J. Senden, A.P. Sheppard, R.M. Sok, A. Limaye, W.V. Pinczewski, and M.A. Knackstedt, "Three-dimensional imaging of multiphase flow in porous media," *Physica A: Statistical Mechanics and its Applications*, vol. 339, Aug. 2004, pp. 166-172.

[5] R.I. Al-Raoush and C.S. Willson, "A pore-scale investigation of a multiphase porous media system," *Journal of Contaminant Hydrology*, vol. 77, Mar. 2005, pp. 67-89.

[6] M. Prodanovic, W. Lindquist, and R. Seright, "Porous structure and fluid partitioning in polyethylene cores from 3D X-ray microtomographic imaging," *Journal of Colloid and Interface Science*, vol. 298, Jun. 2006, pp. 282-297.

[7] J. Bear, *Dynamics of fluids in porous media*, New York: Dover, 1988.

[8] M.A. Celia, P.C. Reeves, and L.A. Ferrand, "Recent advances in pore scale models for multiphase flow in prous media," *Reviews of Geophysics*, vol. 33, pp. PAGES 1049–1058.

[9] M.J. Blunt, "Flow in porous media -- pore-network models and multiphase flow," *Current Opinion in Colloid & Interface Science*, vol. 6, Jun. 2001, pp. 197-207.

[10] S. Bakke and P. Øren, "3-D Pore-Scale Modelling of Sandstones and Flow Simulations in the Pore Networks," *SPE Journal*, vol. 2, 1997.

[11] Lindquist, W. Brent, *3DMA-Rock, a software package for automated analysis of rock pore structure in 3D computed microtomography images.*

http://www.ams.sunysb.edu/~lindquis/3dma/3dma_rock/3dma_rock.html.
[12] A.P. Sheppard, R.M. Sok, H. Averdunk, V.B. Robins, and A. Ghous, "Analysis of rock microstructure using high resolution x-ray tomography," *Proceedings of the International Symposium of the Society of Core Analysts*, Trondheim, Norway: 2006, pp. SCA2006-26.
[13] J.Y. Arns, A.P. Sheppard, C.H. Arns, M.A. Knackstedt, A. Yelkhovsky, and W.V. Pinczewski, "Pore-level validation of representative pore networks obtained from micro-CT image," *Proceedings of the International Symposium of the Society of Core Analysts*, Calgary, Canada: 2007, pp. SCA2007-15.
[14] S. Succi, *The lattice Boltzmann equation for fluid dynamics and beyond*, Oxford ;New York: Clarendon Press ;;Oxford University Press, 2001.
[15] M.L. Porter, M.G. Schaap, and D. Wildenschild, "Lattice-Boltzmann simulations of the capillary pressure-saturation-interfacial area relationship for porous media," *Advances in Water Resources*, vol. 32, Nov. 2009, pp. 1632-1640.
[16] T. Ramstad, P. Oren, and S. Bakke, "Simulation of Two Phase Flow in Reservoir Rocks Using a Lattice Boltzmann Method," *Proceedings of SPE Annual Technical Conference and Exhibition*, 2009.
[17] D. Silin and T. Patzek, "Predicting Relative-Permeability Curves Directly From Rock Images," *Proceedings of SPE Annual Technical Conference and Exhibition*, 2009.
[18] M. Hilpert and C.T. Miller, "Pore-morphology-based simulation of drainage in totally wetting porous media," *Advances in Water Resources*, vol. 24, Feb. , pp. 243-255.
[19] D. Silin, J. Guodong, and T. Patzek, "Robust Determination of the Pore Space Morphology in Sedimentary Rocks," *Proceedings of SPE Annual Technical Conference and Exhibition*, 2003.
[20] M. Prodanovic and S. Bryant, "A level set method for determining critical curvatures for drainage and imbibition," *Journal of Colloid and Interface Science*, vol. 304, 2006, pp. 442-458.
[21] Torres-Verdin, Carlos, *Pore-Level Petrophysics Toolbox (PLPT), http://uts.cc.utexas.edu/~cefe/res/*.
[22] J. Guodong, T. Patzek, and D. Silin, "Direct Prediction of the Absolute Permeability of Unconsolidated and Consolidated Reservoir Rock," *Proceedings of SPE Annual Technical Conference and Exhibition*, 2004.
[23] G. Jin, C. Torres-Verdin, F. Radaelli, and E. Rossi, "Experimental Validation of Pore-Level Calculations of Static and Dynamic Petrophysical Properties of Clastic Rocks," *Proceedings of SPE Annual Technical Conference and Exhibition*, 2007.
[24] Y.H. Qian and Y. Zhou, "Complete Galilean-invariant lattice BGK models for the Navier-Stokes equation," *Europhysics Letters*, vol. 42, May. 1998, pp. 359-364.
[25] N.S. Martys and H. Chen, "Simulation of multicomponent fluids in complex three-dimensional geometries by the lattice Boltzmann method," *Physical Review E*, vol. 53, Jan. 1996, p. 743.
[26] V. Shabro, F. Javadpour, and C. Torres-Verdin, "A Generalized Finite-Difference Advective (FDDA) Model for Gas Flow in Micro- and Nano-porous Media," *World Journal of Engineering*, vol. (to appear), 2010.
[27] V. Shabro, F. Javadpour, C. Torres-Verdin, and S.B. Fomel, "Diffusive-Advective Gas Flow Modeling in Random Nano-Porous Systems (RNPS) at Difference Knudsen Regimes," *Proceedins of the 17th International Conference of Composites or Nano-Engineering*, 2009.
[28] M. Prodanovic and S. Bryant, "Physics-Driven Interface Modeling for Drainage and Imbibition in Fractures," *SPE Journal*, vol. 14, 2009.
[29] Prodanovic, Masa, *Level Set Method based Progressive Quasi-Static (LSMPQS) software. http://users.ices.utexas.edu/~masha/lsmpqs/index.html*.
[30] C.H. Arns, M.A. Knackstedt, M.V. Pinczewski, and W.B. Lindquist, "Accurate estimation of transport properties from microtomographic images."
[31] M. Kumar, "Multiphase flow in reservoir cores using digital core analysis," Australian National University, 2009.
[32] M. Prodanovic, S. Bryant, and Z. Karpyn, "Investigating Matrix-Fracture Transfer via a Level Set Method for Drainage and Imbibition," *Proceedings of SPE Annual Technical Conference and Exhibition*, 2008.